

THE 1980 LOW STATE OF AM HERCULIS

DAVID W. LATHAM,¹ JAMES LIEBERT,² AND JOÃO E. STEINER^{1,3}

Received 1980 October 2; accepted 1980 December 24

ABSTRACT

We report a series of phase-dependent spectrophotometric observations at optical and near-infrared wavelengths of AM Herculis during its low state (1980 June–September); broad-band circular polarization results are discussed as well. Several separate components of the continuum and emission-line radiation are discussed:

1. A strongly polarized optical continuum is still present, with an amplitude in red light as high as -11% , despite the dilution by photospheric radiation from both the primary and secondary stars. The polarization curve differs markedly from earlier high state observations, but resembles more closely the 1979 data of Bailey and Axon.

2. Weakened, much narrower emission lines of hydrogen, He I, He II, and low excitation transitions appear consistently on our spectra. The radial velocities generally fit the peak component previously identified geometrically with the secondary star in high state spectra. However, on one night we observed much broader, stronger emission lines showing additional peak components with much different radial velocities, though they do not correspond to the high-state radial velocity curve of the broad component. We attribute the extra line radiation to a special accretion episode, probably associated with the normally less-active magnetic pole. The underlying photospheric features appear somewhat masked during the times of enhanced line emission.

3. The dwarf M secondary star spectrum in the near-infrared generally fits spectral type M4.5–5 V, showing only marginal variations with orbital phase. The spectral type and photometric parallax are generally consistent with earlier inferences of Young and Schneider. The illuminated side of the secondary is viewed most directly following magnetic phase zero.

4. The blue spectrum is dominated by strong, complicated absorption features of hydrogen Zeeman components. While 13 megagauss is the dominant surface field strength represented at all phases, there are pervasive features which require either magnetic field strengths near 20 megagauss for hydrogen components or a variable and ad hoc contribution from neutral helium components. Aside from the masking due to enhanced accretion events, there are also phase-dependent variations in the positions and strengths of the Zeeman absorption, in both the blue and red spectra. Thus, the spectrum cannot be explained by a simple heated polar spot model. However, there are complications beyond a simple centered dipole interpretation as well: We find a strong contribution from apparent 20 megagauss components near phase zero, yet this seems incompatible with the AM Her geometry previously inferred from the phase dependence of linear polarization and X-rays. We suggest that He II 4686 Å absorption complicates the spectrum in the 4600–4700 Å region; this is compatible with temperature estimates from *IUE* data. Finally, a vertically offset dipole geometry with the higher field pole visible near phase zero may reconcile the geometric difficulties.

Subject headings: polarization — stars: emission-line — stars: individual — stars: magnetic — spectrophotometry — X-rays: binaries

I. INTRODUCTION

While all nova-like binaries (e.g., Robinson 1976) may have variations in their mass transfer rates, the consequences of these variations for the magnetic AM Her

objects are particularly interesting. It is generally believed that the transferred gas in these objects is controlled by the primary white dwarf's magnetosphere soon after it leaves the secondary so that no accretion disk is formed (Chanmugam and Wagner 1977; Stockman *et al.* 1977). The gas follows the field lines and impacts directly on the primary near a magnetic pole. The primary must avoid being spun up by angular momentum transfer so that its field geometry remains

¹Harvard-Smithsonian Center for Astrophysics, Cambridge.

²Steward Observatory, University of Arizona, Tucson.

³On leave from IAG-Universidade de Sao Paulo, C.P. 30627, S. Paulo, Brazil.

phase-locked with the binary period. Optical continuum radiation in AM Her objects is normally believed to be dominated by polarized cyclotron radiation in the hot accretion stream approaching polar impact. Ultraviolet, soft and hard X-radiation is emitted near the pole as well (e.g., Hearn and Richardson 1977; Lamb and Masters 1979). Thus, without the accretion disk—the dominant light source in most quiescent cataclysmics and a storage bin for previously transferred gas—the luminosity of an AM Her binary may drop rapidly when the mass accretion rate is low. If the gravitational energy from accretion is reduced enough, the low state in an AM Her object may afford the opportunity to observe photospheric radiation from the secondary or primary. In any case, the physical parameters and geometry of the reduced gas stream are likely to change with the mass transfer rate.

The low state properties of the prototype AM Her have not been well studied, despite the fact that Bond and Tift (1974) first identified the object as a 15th magnitude nova-like variable when it was at a relatively low brightness. Yet, when Tapia (1977a) discovered unprecedented strong linear and circular polarization in the optical radiation, following Berg and Duthie's (1977) association of AM Her with an Uhuru X-ray source, the star was generally at 12–13th magnitude. Subsequent spectroscopic studies consistently showed strong, broad H, He II, He I and high ionization emission lines of C III, N III, C IV generally at all phases in the spectrum (Crampton and Cowley 1977; Stockman *et al.* 1977; Greenstein *et al.* 1977). Raymond *et al.* (1979) reported a rich ultraviolet spectrum including C IV and N V emission. Yet, Feigelson, Dexter, and Liller (1978) had documented from the Harvard plate collection that AM Her has generally varied between about 12th and 15th magnitude long-term states over the last 90 years.

VV Pup, on the other hand, is an AM Her-type object (Tapia 1977b) which has been studied in a low, ~18th magnitude state. A red color excess appeared which was most likely due to the secondary star in that system (Liebert *et al.* 1978). A year later, when VV Pup was at an intermediate brightness (~17th magnitude), absorptions convincingly attributable to cyclotron high harmonics were found (Visvanathan and Wickramasinghe 1979a, b; Stockman, Liebert, and Bond 1979). However, the VV Pup field strength of only 3.1×10^7 gauss was considerably below the general estimate of 10^8 gauss fields for the AM Her objects. Thus, the report by Mattei (1980) that AM Her had dipped once again to magnitude 15.0–15.5 created the first opportunity since its discovery for a concerted study of its quiescent behavior.

II. THE OBSERVATIONAL BASE

We report here a series of spectrophotometric scans obtained with the Smithsonian-Arizona 4.5 m Multiple

Mirror Telescope (MMT) and with the Steward 2.3 m reflector. Broad-band polarimetry obtained with the 2.3 m reflector are also discussed. All observations were obtained between 1980 June 15 (UT) and September 5, during which time the object was apparently in a consistent low state near 15th magnitude. Ultraviolet observations with the *International Ultraviolet Explorer* (IUE) satellite were also obtained on June 30 (Raymond 1980, private communication).

An observational log of all individual scans is presented in Table 1. Heliocentric phases were computed using Tapia's (1977a) epoch and Young and Schneider's (1979) improved period. Magnetic phase zero coincides with a pulse of linear polarization, though this may be absent for periods of time, and is the approximate time for zero crossing (negative-to-positive sign) of the circular polarization (see figures in Crampton and Cowley 1977).

The new MMT spectrograph and photon-counting Reticon detector are described in Angel, Hilliard, and Weymann (1979) and Latham (1979), respectively. The image tube configuration used a Varo front end which provided generally red wavelength sensitivity. The 1.75 slit width and 600 line mm^{-1} grating in second order allows a spectral resolution of about 4 Å. The 2.3 m Steward analog Reticon system is described in Hege, Woolf, and Cromwell (1979). A Varo image tube package and 600 line mm^{-1} grating were also employed, but in first order with a spectral resolution of only 9–10 Å.

In Figure 1, the basic low state spectrum of AM Her (the sum of all MMT blue spectra covering 4200–5100 Å) is displayed. The spectrum covering ~5350–7350 Å is our only MMT red spectrum, obtained at UT 15 June 0912. We shall show in this paper that there are three identifiable components to the optical continuum and two (or more) line radiation components in the AM Her low state. Each will be discussed in detail in the following sections. They are:

1. A strongly polarized optical continuum is still present, as shown by the broad-band polarimetry in § III. In the high state, this continuum source shows no obvious absorption features. However, while the polarized light evidently has a red optical color, it is unlikely that it follows the ν^{-1} power law which fits the total energy distribution from the IUE ultraviolet to about one micron (Stockman *et al.* 1977; Raymond *et al.* 1979; Fabbiano *et al.* 1981).

2. Weakened, much narrower emission lines of hydrogen, and very weak He I and He II lines are present in our spectra. The high excitation C–N 4640–4650 blend is only identified in a few scans when He II is strong, though magnetic absorption has badly distorted the continuum. Low excitation lines of Fe II are present, however. While the narrow emission lines generally fit the narrow or peak line component in the normal AM Her spectrum, we also observed stronger and broader

TABLE 1
SPECTROSCOPIC OBSERVATIONAL LOG

Date (UT)	File No.	MST (mean)	Duration (min)	Phase	Remarks
MMT Observations					
1980 Jun 15	172	01:47	20	0.794	...
	173	02:12	20	0.929	red spectrum
1980 Jun 17	184	00:26	20	0.867	cloudy
	185	00:50	20	0.056	...
1980 Jun 18	196	23:21	10	0.273	cloudy
	197	23:37	10	0.359	...
	201	23:50	10	0.429	heavy clouds
	202	00:07	10	0.521	...
	203	00:22	10	0.601	...
	204	00:36	10	0.677	...
	205	00:46	10	0.731	...
	206	01:01	10	0.812	...
	207	01:11	10	0.865	...
	208	01:28	10	0.957	clouds
	209	01:47	10	0.059	...
	210	02:03	10	0.146	...
	211	02:19	10	0.232	...
	212	02:35	10	0.318	...
	213	02:47	10	0.383	...
214	03:07	10	0.490	...	
215	03:18	10	0.549	clouds	
1980 June 19 ...	228	00:05	10	0.266	clouds
	229	00:48	10	0.535	...
	230	01:04	10	0.583	...
2.3 m Observations					
1980 Jul 2	16	01:38	8	0.599	yellow tilt
	17	01:46	8	0.642	yellow tilt
	18	01:57	8	0.701	red tilt, clouds
	19	02:10	8	0.771	red
	20	02:20	8	0.825	red, heavy clouds
	24	03:17	17	0.132	red, heavy clouds
	26	04:06	8	0.396	red, light clouds
	27	04:15	8	0.444	red
1980 Sep 5	1656	00:02	15	0.240	red
	1818	01:23	10	0.681	red
	1836	01:36	9	0.747	yellow

line emission on one occasion which did not fit the radial velocity curves of either the normal narrow or broad AM Her components.

3. A late-type secondary star spectrum with TiO bands and other normal features is easily seen at wavelengths longer than 6000 Å. Its general properties are consistent with the inferences of Young and Schneider (1979) from high state observations.

4. A detailed, complicated absorption spectrum, obviously due to Zeeman components of hydrogen lines, is the principal discovery of the low state observations. We show in § VI that the surface fields represented may cover ~13–20 magagauss, field strengths far lower than those previously inferred from the amplitudes of linear and circular polarization in AM Her and from attempts

to model the phase-locked mass transfer. Similar observations and accompanying spectropolarimetry have independently been obtained at the Lick Observatory (Schmidt, Stockman, and Margon 1981), leaving no doubt as to the general interpretation of the magnetic features.

III. THE POLARIZED CONTINUUM RADIATION

Broad-band circular polarization measurements were obtained on June 21 (UT) by H. S. Stockman. The coverage included approximately 5400–8500 Å, with the blue end cut by a blocking filter and the red end limited by the tube response. Slightly more than one 3.09-hour period was covered before the observations were stopped

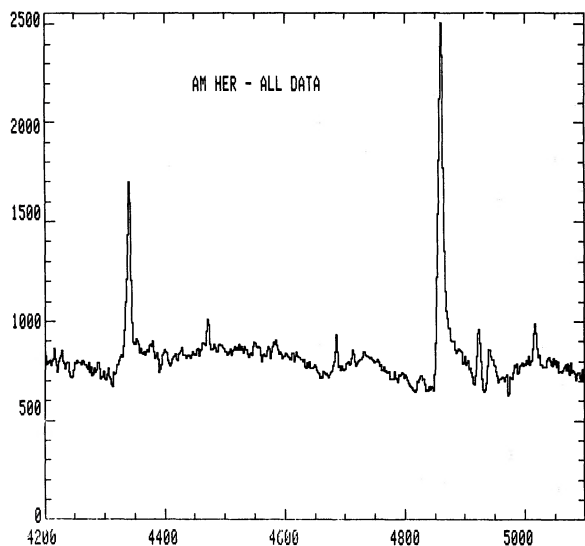


FIG. 1a

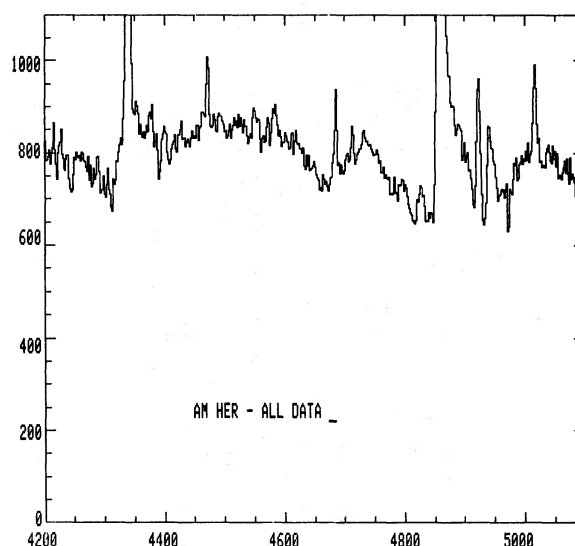


FIG. 1b

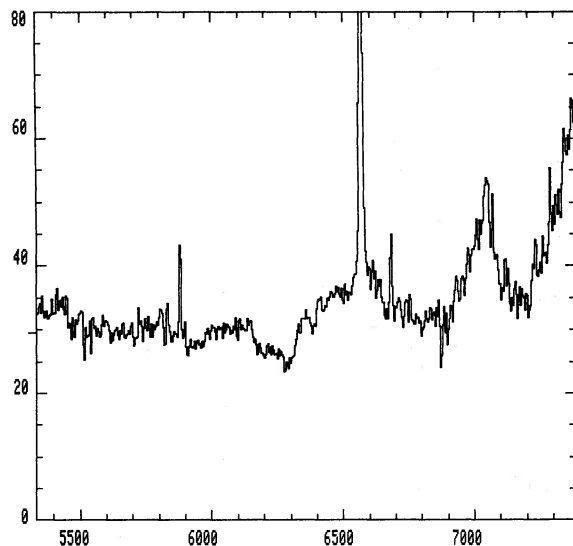


FIG. 1c

FIG. 1.—(a) Sum of all MMT blue wavelength scans; (b) the same sum scaled to show the continuum and absorption features; (c) the MMT red wavelength scan.

by the onset of clouds. We do not present a light curve due to these marginal conditions.

In view of the drastically reduced optical energy output and the evidence for strong primary and secondary star absorption features, it is very surprising to report a maximum circular polarization exceeding 11%—larger than the maximum amplitude originally reported in Tapia (1977a) and other early observations (e.g., Stockman *et al.* 1977; Stockman and Sargent 1979). We show the individual data points in a series of eight, spaced 1 1/2 minutes apart, along with the original

curve taken from Tapia's (1977a) Figure 2. The recent data exhibit only a small excursion to positive polarization, though the positive zero-crossing is very close in phase to the Tapia crossing. However, the detailed shape resembles more closely the 1979 data from Bailey and Axon (1981)—the dashed curve in Figure 2—taken also when the object was in a high state. In view of the drastic changes in the polarization curves of VV Pup between high and low states, the similarity of the recent AM Her curves is most remarkable.

That the circular polarization is even the same sign at various phases compared with previous data convincingly shows that the same source of polarized continuum emission—presumably, a cyclotron funnel—remained active in this quiescent state. If this process were completely absent in the faint AM Her, one would not observe negatively polarized light for most of the period but, presumably, positive polarization of a much reduced amplitude—for a 20 megagauss polar field, the continuum should be polarized <1% (Angel 1978; Landstreet 1979).

Given that the cyclotron polarization source is still present, its reduced light output must be compensated for by a drastic increase in the percentage of circularly polarized light emitted. This is expected if the optical depth of this region is much smaller in the curtailed gas flow. An elementary calculation indicates that, if the polarized continuum source were 100% polarized at phases near 0.27 and 0.77, the cyclotron source must contribute at least 10% of the total light in the bandpass covered by the polarimetric observations. Given the dominance of the secondary redwards of 7000 Å (§ V), it is likely that the polarized source contributes mainly in the shorter wavelengths of the bandpass.

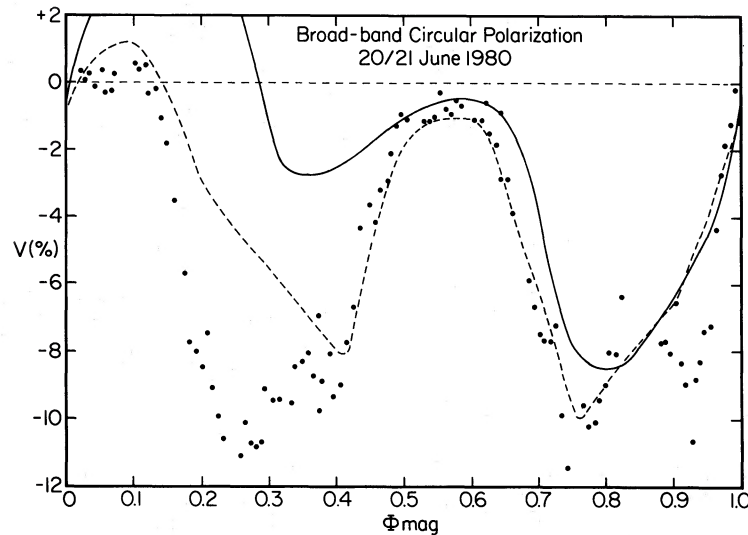


FIG. 2.—Circular polarization curve (5400–8500 Å) for AM Her during its low state (*filled circles*), obtained by Dr. H. S. Stockman with the Steward 2.3 m reflector. The solid curve is an approximation of Tapia's (1977*a*) data; the dashed line is a schematic of the 0.68 μ data of Bailey and Axon (1981) during a more recent high state. The magnetic ephemeris was computed using Tapia's epoch and the refined period of Young and Schneider (1979).

IV. THE EMISSION-LINE RADIATION

The high state AM Her spectrum exhibits strong and broad emission lines, with excitations as low as Fe II in the optical and as high as C IV and N V in the ultraviolet. Phased observations of the optical lines have resulted in the identification of a broad base component and a narrow peak component, differing in their radial amplitudes and phasing (Crampton and Cowley 1977; Greenstein *et al.* 1977). Since the Balmer decrement of the narrow component is much closer to recombinational, it was logical to associate it with the region near the secondary star. The He II narrow emission-line equivalent widths were shown to be consistent with Case B recombination from the expected extreme-ultraviolet flux (Fabbiano *et al.* 1981). Young and Schneider's (1979) identification of Na I λ 8192 absorption, typical of a late-type M dwarf with the amplitude and phasing of the narrow emission component, conclusively placed this component near the secondary star in the system. However, the great widths and pressure effects associated with the broad component, as well as the different velocity curve, tended to locate it much farther down the accretion stream, perhaps near the top of the funnel.

The narrow emission-line component was consistently present in our low state AM Her spectra, and the broad component was generally absent. The Balmer line ratios on the MMT blue and Steward red scans were generally recombinational. However, on the night of June 18, for which a large fraction of our total MMT scans were taken, a transient accretion event evidently occurred which enhanced the emission-line strengths and com-

plicated their profiles. Hence, we divide the discussion of the emission line properties into two parts: (a) the normal phase-dependent properties, and (b) the June 18 transient accretion episode.

a) Phase-Dependent Properties and Radial Velocities

In Figure 3, we have averaged all MMT scans within intervals of 0.2 in phase to show the phase-dependent changes in the emission lines. On each individual scan, we measured equivalent widths and full widths at half-maximum (FWHM); the H β and H γ values are plotted against phase in Figure 4. If we disregard the June 18 data, there is no clear dependence of the Balmer line strengths and widths with phase. In all the data, there is a correlation of equivalent width with FWHM—§ IV*b*. The weak He II and He I lines were present at all phases. In Table 2 average line parameters are presented for the quiescent AM Her scans (omitting those on June 18). Despite the relative weakness of the helium lines, the ratio of He II/He I strengths is not unlike that in the high state. This suggests that the extreme ultraviolet flux source normally responsible for the recombination radiation (Fabbiano *et al.* 1981) is still present, albeit at a much reduced level. If we use the previous correlation between the observed He II/H β ratio and the UV/soft X-ray temperature, we infer a UV component temperature of about 8–10 eV at minimum. No soft X-rays are predicted. Hard X-rays should appear during the accretion episodes, such as that discussed in the following subsection.

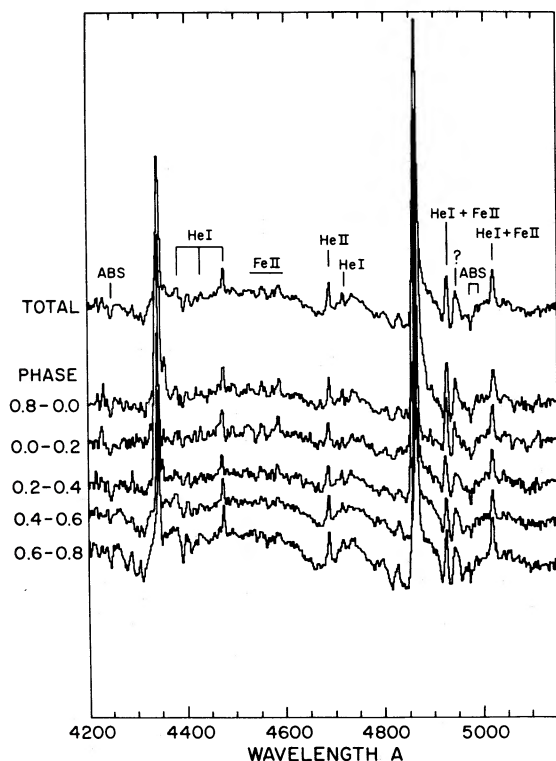


FIG. 3.— Separate sums of MMT scans, grouped in intervals of 0.2 in magnetic phase. Low and high excitation emission lines, discussed in § IV, are identified on the blue spectra. The sharp absorption features near 4970–4990 Å may be due to field-insensitive Zeeman transitions, as discussed in § VI. The peculiar rise near 4950 Å may be due in part to a TiO bandhead in the secondary star and to magnetic absorption in the primary. The absorption near 4250 Å, persisting throughout all phases, is not identified here.

The blue spectrum is also sprinkled with blends of Fe II, particularly multiplets (37) and (38). Two Fe II lines near 4923 Å and 5018 Å are blended with He I lines. The strengths of the low excitation lines clearly correlate with phase in that they are strongest near phase zero and weakest near phase 0.5. It is logical to interpret the low excitation lines as arising from resonant fluorescence excited by the primary's hard ultraviolet component on the heated side of the secondary's envelope. This emission region may be partially eclipsed during the part of the binary period when we are viewing primarily the back side of the secondary. That the hydrogen and helium lines are not obviously eclipsed indicates that the higher excitation gas covers a more extended volume, though the radial velocities discussed next still would place it in the vicinity of the secondary star.

On individual scans, we measured line positions in three different ways: (1) at the line peak or peaks, (2) at the FWHM level, and (3) near the base, about 10%

above the estimated continuum.⁴ Except for the scans affected by the June 18 transient, we noted no significant difference between the radial velocity curves as measured in the three different ways. We also searched for an underlying broad component by constructing a crude Boroson-Greenstein contour diagram (Greenstein *et al.* 1977). The results confirm the lack of any clear phase-dependent profile or strength changes (Fig. 3) and indicate that a single-line component generally was present. In Figure 5, we show only the data measured at the Balmer line peaks, with the June 18 data identified by the filled and open circles. Most of the scans obtained on June 18 showed stronger and broader lines (Fig. 4) with complicated profiles. In particular, two or more significant peaks could generally be measured in these data. Inspection of Figure 5 leads us to conclude that the lowest velocity peak in each of these cases can be identified with the velocity curve of the normal, narrow component, while the other peaks are associated with transient-event gas at much different velocity in the system. The self-consistency of this interpretation was tested by lumping the June 18 low velocity peaks with the data for the other nights in calculating our radial velocity solution. (We did not attempt to exclude the June 18 data entirely in the radial velocity solution because of lack of coverage for phases <0.5.) The fit to

$$V = \gamma + K \sin(\theta - \phi)$$

yielded $K = 100 \text{ km s}^{-1}$, $\gamma = -57 \text{ km s}^{-1}$, with ϕ the positive zero-crossing at phase 0.42. This solution is similar in amplitude and phasing to the narrow component previously identified by Crampton and Cowley (1977), Greenstein *et al.* (1977), and Young and Schneider (1979). The more difficult He I 4471, He II 4686 and Fe II 4582 lines were measured on phase-averaged spectra. These generally follow the mean curve of the hydrogen data. The 2.3 m red spectra lack sufficient resolution to compare the radial velocities of secondary star absorption features with the narrow emission-line component.

b) Enhanced Emission Lines on June 18: An Accretion Episode

We illustrate the anomalous emission-line behavior observed on June 18 by the pairs of H β profiles shown

⁴The existence of magnetic absorption features overlapping the emission greatly complicates the definition of a continuum from which line parameters could be measured, and it can distort line profiles markedly. This problem is addressed in detail in § VI. For now, we note that only the region some 10–40 Å redward of the H β line peak could be used as a continuum for this line, since this lies generally between the π and σ^+ components, though it is complicated by phase-dependent magnetic effects, and weaker emission lines as well. For H γ the blending problem is even worse, and often no true continuum exists near the line.

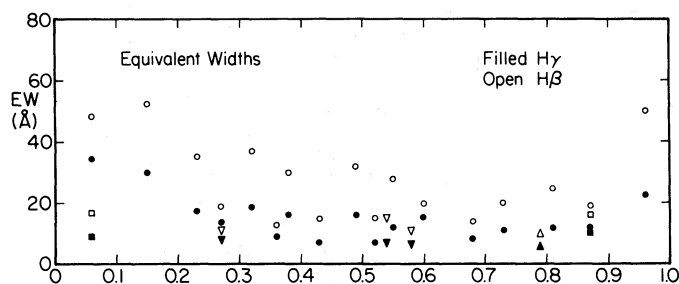


FIG. 4a

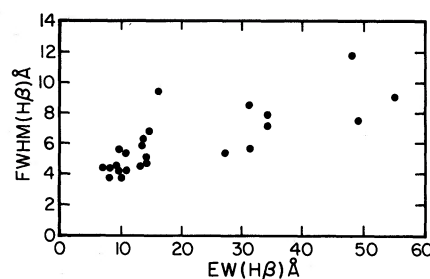


FIG. 4b

FIG. 4.—(a) Equivalent widths for the hydrogen lines in the blue MMT spectra plotted against magnetic phase. Since the line strengths at most phases were greater on the night of June 18 (UT), these measurements are marked by circles, June 17 scans by squares, June 15 scans by triangles with the bases down, and June 19 observations by base-up triangles; (b) the FWHM values for all scans are plotted against the equivalent widths for $H\beta$. The lowest FWHM values are limited by the instrumental resolution.

at similar phase in Figure 6. The substantially stronger emission lines, skewed profiles with multiple peaks, and greatly enhanced widths indicate that gas was temporarily excited at velocities much different from that for the secondary star. The strongest line activity occurred on MMT File 208; these extreme line parameters are listed in Table 2. However, the strengths and profiles observed on June 18 were highly variable.

If we consider the data as a whole, there was a clear correlation between the equivalent widths and FWHM values (Fig. 4). For example, the equivalent width of $H\beta$ varied between about 10 Å and 50 Å; the FWHM varied between about 4 Å and 12 Å. While we cannot report the continuum level to which the star may have brightened during these times of enhanced line emission due to continual clouds, the Zeeman absorption features appeared significantly weaker on many scans taken on June 18, especially File 208 (see Fig. 7). It is logical to suppose that the underlying primary photosphere was masked by an enhancement of the polarized continuum source, far down in the accretion stream.

The accretion episode properties detailed above strongly suggest that the line enhancement may be due

to the temporary resurrection of the mechanism producing the broad emission-line component. However, the radial velocities of the additional peaks (Fig. 5) and the additional base emission in general do *not* correspond at all to the high-state, broad-component radial velocity curve. In fact, the strongest additional line emission observed on File 208 occurred up to 1000 km s⁻¹ lower in velocity than the narrow-peak component position. Yet, at phase 0.96 the normal high-state broad component velocity is near maximum *positive* amplitude. Likewise, the additional peaks appearing on other June 18 scans were generally opposite in velocity to the normal broad component.

Since the enhanced line emission was far out of phase with the high-state broad component, the logical supposition is that enhanced accretion occurred to the magnetic pole *opposite* the generally active pole in AM Her. In the source geometry picture advocated by such authors as Lamb (1976) and Tuohy *et al.* (1981), this would be the non-X-ray emitting pole visible only during the X-ray eclipse following phase 0. Other authors have previously suggested that both poles can accrete and emit radiation in AM Her. We defer further discus-

TABLE 2
SOME EMISSION LINE PARAMETERS

LINE	THE QUIESCENT AM HER ^a			DURING ENHANCED ACTIVITY (File 208)		
	Equivalent Width (EW)	FWHM	Full Width ^b Near Base	EW	FWHM	FWB
Hγ 4340.....	9 Å	3.9 Å	8.7 Å	33 Å	9.1 Å	27 Å
Hβ 4861	14	4.7	11.9	50	11.2	35
He I 4471	0.5	4	...	1.4	~7	20?
He II 4686 ...	0.6	3	...	1.0	~7	...
Fe II 4582 ...	0.3	3	...	≲1

^aExcludes June 18 (UT) data.

^bEstimates uncertain due to difficulty in finding the true continuum.

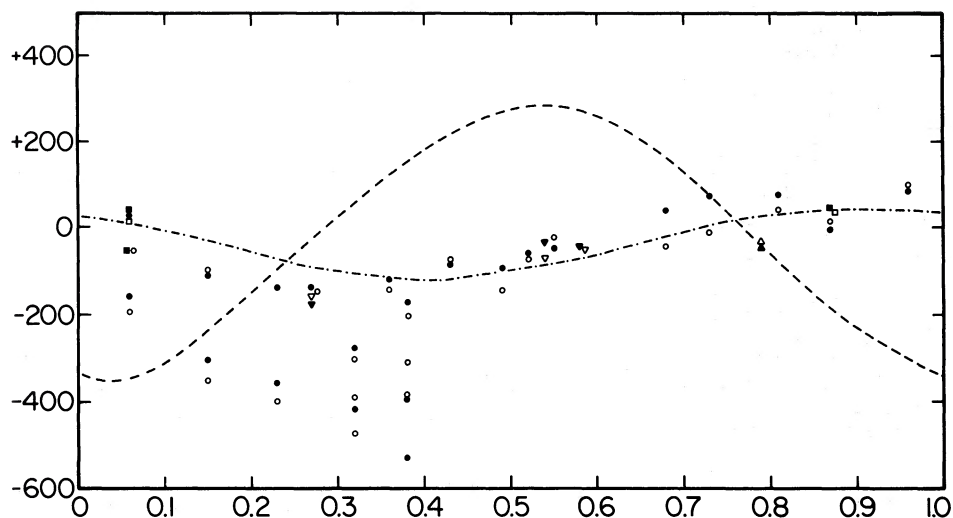


FIG. 5.—Radial velocities of one or more significant peaks for each blue MMT hydrogen-line observation plotted against magnetic phase. The symbols follow the same code as in Fig. 4. The dashed curve and dash-dot curve are the broad and narrow emission-line curves, respectively, from Greenstein *et al.*'s (1977) high state observations—their Fig. 4.

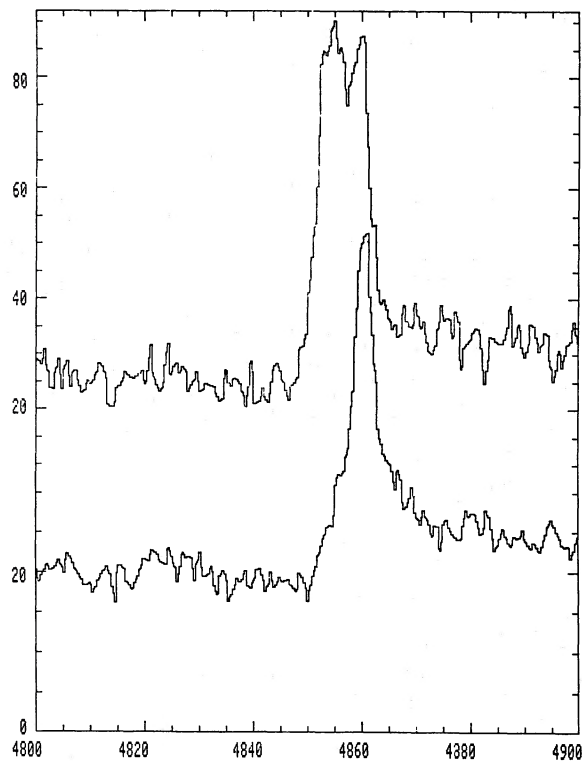


FIG. 6a

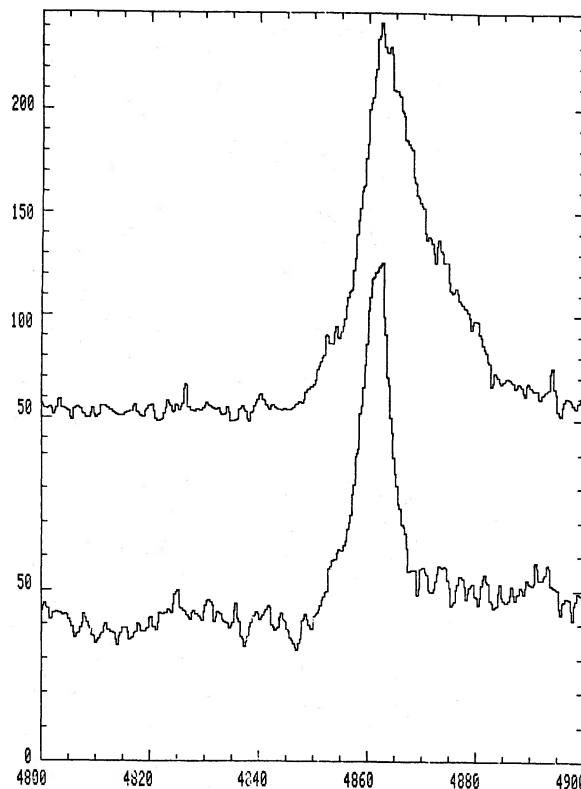


FIG. 6b

FIG. 6.—Two pairs of $H\beta$ line profiles at similar magnetic phases. (a) MMT files 203 and 230, taken at phases 0.58 and 0.60 on two separate nights; (b) MMT files 207 and 208, consecutive observations on June 18, separated by 0.09 in phase. These pairs illustrate the importance of “accretion episodes” having no clear relationship to binary phase on the line strengths, profiles, and radial velocities.

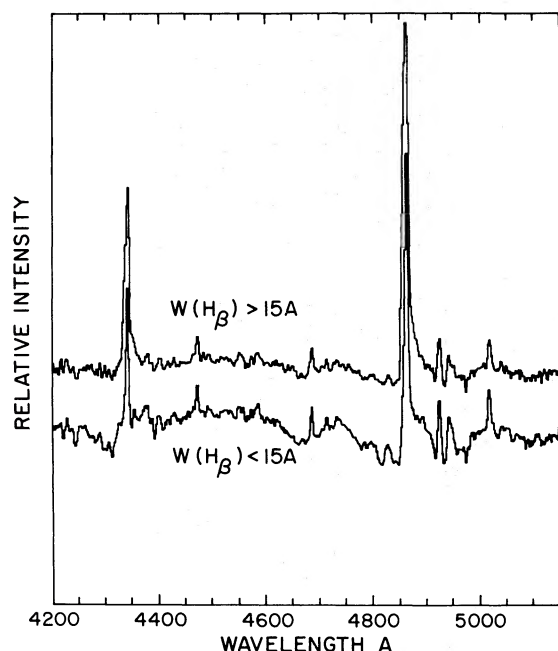


FIG. 7.—The masking of the photospheric Zeeman features during scans showing abnormally strong line emission (i.e., accretion episodes). Most scans used for the top sum occurred on June 18. Both sums have the same intensity zero point at the bottom of the figure.

sion of the source geometry to § VI. However, it should be noted in conclusion that complicated emission-line structure inconsistent with a simple two-component model has been reported in other AM Her objects: Crampton, Hutchings, and Cowley (1981) found that 2A0311-227 shows puzzling, complex, narrow-line components at some phases. Schneider and Young's (1980) line profiles for VV Pup exhibit doubled peaks over limited intervals of phase.

V. THE SECONDARY STAR

In addition to the single MMT red wavelength observation (Fig. 1), we obtained several scans with the Steward 2.3 m reflector (Fig. 8 and Table 1). The energy distributions for the July observations are in error due to instrument alignment difficulties.

It is obvious from Figure 8 that the secondary star is a late M dwarf, as established by Young and Schneider (1979), and that it contributes significantly redward of 5500 Å and totally dominates the energy distribution past 7000 Å. Since classical spectroscopic classification techniques have now been extended to near-infrared wavelengths (Boeshaar 1976), we have employed these techniques to classify the object and to look for variations in the absorption spectrum with binary phase. Two spectroscopically normal old-disk dwarfs (Boeshaar

1980) were observed along with AM Her to facilitate comparison on the same low resolution instrumental system (Fig. 8). Absorption features used included: (1) the shape of the pseudo-continuum region at 7300–7600 Å, which is increasingly eaten away on its blue side for later types; (2) the continuum flux ratios 8050 Å/7400 Å, for comparison with narrow-band fluxes from O'Connell (1973); (3) the onset of VO bands at 7850–7982 Å, which occurs for M5 and later; (4) the strengths of K I lines at 7765 and 7699 Å; and (5) the strengths of the Na I 8183 and 8195 Å somewhat blended at this resolution.

The classifications for each of these features of the mean September observations are M4–5, M4.5, M3.5–4, M3?, and M5, respectively. We note that the K I lines do not appear distinctly in AM Her and are very likely filled in with emission, unlike the nonresonant Na I lines. Thus we discard the M3? classification (No. 4 above). While the hot, primary photosphere component should contribute no more than 10% of the light at 8000 Å and is easily allowed for in this classification exercise, the residual polarized-light source (§ III) poses a more serious problem. In the high state, this source is known to be fairly red ($f_p \sim \nu^{-1}$), though not nearly as red as the M dwarf. If the polarized source does not get significantly redder at lower luminosities, it follows that the long wavelength features are least affected by the other components. Hence, we continue to favor the M4.5–M5 classification, as used in Schmidt, Stockman, and Margon (1981) for an estimate of the photometric parallax. This agrees closely with the high state Na I line observations of Young and Schneider (1979).

The strengths of these absorption features vary less than a full subtype with binary phase for coverage including roughly each 0.25 interval in phase. While the energy distribution appears one-half subtype redder at phase 0.24 than at 0.68 in the September scans, we cannot use the July data at other phases for this purpose. Now one expects from both the radial velocity arguments (Young and Schneider 1979) and the marked variations in Fe II emission that one is viewing more of the illuminated side of the secondary star near phase 0.1; one might then expect the backside near phase 0.65 to be cooler and possibly later in spectral type. There are, however, only marginal differences in the five classification features outlined previously. The most likely changes in the absorption spectrum are the deepening of the absorptions near 5892 Å and 6300 Å near phase zero. The first feature is the Na I D blend, whose weakness presumably results from filling-in due to Na I emission, consistent with the behavior of the Fe II lines. The 6300 Å absorption minimum is attributed to H α Zeeman absorption in the primary; its phase-dependent changes are consistent with changes in blue spectra discussed in § VI.

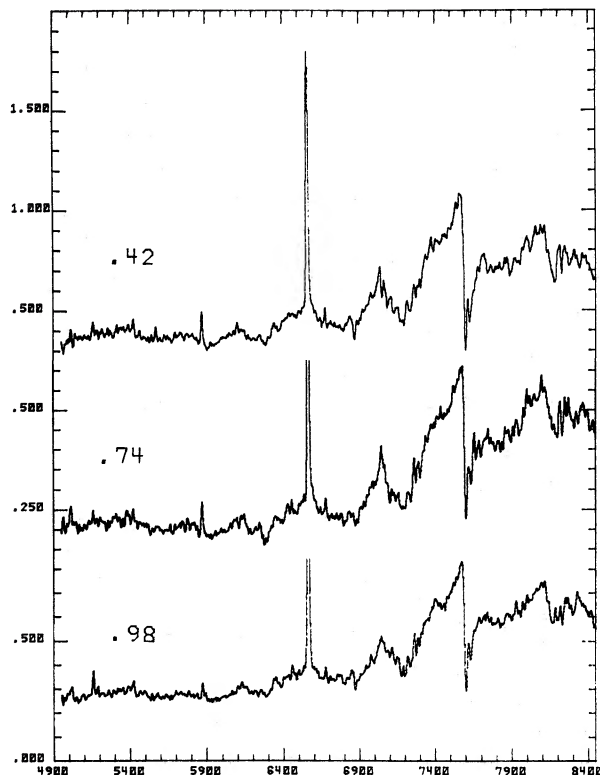


FIG. 8a

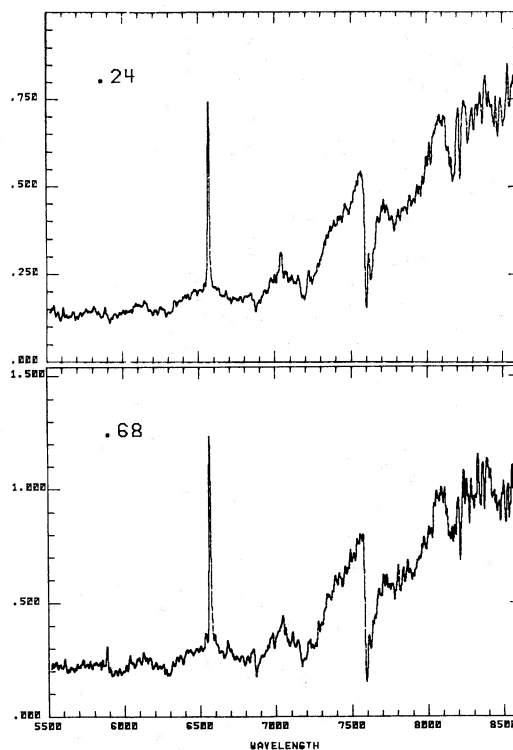


FIG. 8b

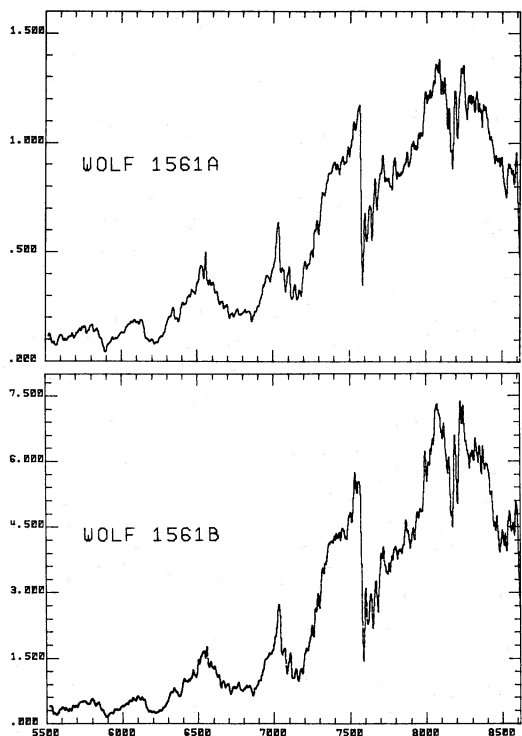


FIG. 8c

FIG. 8.—Red observations obtained with the Steward 2.3 m telescope and Reticon spectrophotometer. (a) July scans for phases 0.42, 0.74, and 0.98, respectively. The energy distributions are badly in error longward of 7500 Å; (b) September scans of AM Her at phases 0.24 and 0.68; (c) Comparison scans in September of Wolf 1561A (an M4 V star) and Wolf 1561B (an M5 V companion). Absorption features used for classifying AM Her are discussed in § V.

VI. THE MAGNETIC WHITE DWARF PHOTOSPHERE

The striking hydrogen Zeeman features are readily identifiable in the time-averaged spectrum shown in Figure 1b. In particular, the three broad minima in the continuum near the $H\beta$ emission line—two blueshifted from rest and one redshifted—may be recognized as blends of σ_- , π , and σ_+ $H\beta$ absorption components in the presence of a field strong enough to have a significant quadratic shift (blueward), in addition to the linear triplet splitting. In fact, its general appearance is like the spectra of known magnetic DA white dwarfs, such as GD 90 (Angel *et al.* 1974) or BPM 25114 (Wickramasinghe and Martin 1979a). The appearance of strong H absorption may only constrain the mean temperature of the absorbing region to something like 8000–40,000 K. Yet it is quite clear that its origin must be completely different than the cause of the equally striking cyclotron absorption features observed in VV Pup at a low brightness level (Visvanathan and

Wickramasinghe 1979*a*; Stockman, Liebert, and Bond 1979). Instead of an extremely high temperature ($T \sim 10^7$ K) spot in the accretion column—necessary for opacity at high cyclotron harmonics—this continuum radiation and absorption must originate over a fairly extended region, almost certainly the surface of the primary. Certainly, the sharpness of the specific, field-insensitive σ_+ Zeeman components discussed subsequently precludes the kind of velocity broadening expected if an extended surface area of an accretion stream were the source of the absorption. Hence, we can assume that the Zeeman absorption allows determination of the primary's surface magnetic field strength. We note that the field range of 13–20 megagauss apparently required to fit the Zeeman features is substantially lower than previous inferences (Tapia 1977*b*) but was predicted theoretically (Lamb 1979). The implications are discussed in Schmidt, Stockman, and Margon (1981).

The match of the secondary star's red spectrum to an M4.5 dwarf predicts that its light contribution is less than 30% at 5000 Å. With the possible exception of the TiO $\lambda 4960$ bandhead, no detectable absorption features from this component should be seen in the MMT spectra. Indeed, contrary to Patterson (1980), there is no evidence for late-type absorption features such as Ca I $\lambda 4226$; the absorption near $\lambda 4300$ is entirely attributable to the π component of H γ absorption, and not the CH G band. We work with the hypothesis that Zeeman components can account for all observed absorption features in the blue spectrum, including some noticeably sharp dips in Figures 1 and 3.

It is misleading to attempt an estimate of the photospheric temperature from any part of the optical energy distribution. The Zeeman features blanket most of the blue spectrum, and there is every reason to expect their opacity to increase in the optical ultraviolet (see Greenstein and Boksenberg's (1978) analysis of the isolated magnetic white dwarf Feige 7). On the other hand, Raymond's (1980, private communication) discovery of strong Ly α absorption indicates that the photospheric source may contribute strongly to the IUE continuum: He fits a temperature in the 30,000–100,000 K range from the averaged energy distribution. We thus may expect strong transitions of He II and He I to be potential contributors to the Zeeman spectrum, though the possible contributions of heavier elements in the optical spectrum are quite limited at these high temperatures, unless the composition were quite enhanced in certain elements. One can presume, however, from the results of white dwarf atmospheric modeling, that the Balmer opacity would dominate for a Population I composition gas.

Studies of isolated magnetic white dwarfs have revealed examples with apparently dipolar field geometries. If the entire surface of the star contributes to the observed light, a wide range of field strengths would be

represented in the Zeeman features, spanning a factor of 2 if the field were dipolar. In this case, the observed Zeeman spectrum would generally vary with orbital phase, depending on the viewing geometry. However, the continued deposition of accretion energy just near the magnetic pole(s) suggests that this region might be hotter than the rest of the photosphere and could dominate the optical and ultraviolet radiation. Alternatively then, the Zeeman spectrum might fit a small spread in field strength close to the polar value; only small variations with binary phase would be expected, unless the polar cap is eclipsed. Finally, the situation could be much more complicated if the stellar field were more complex than a dipole, or if there were temperature or composition variations.

We thus begin by testing the detailed Zeeman spectra against the two simplest hypotheses: (1) that the radiation is confined to polar spots having a restricted range of field strength, with small orbital phase changes; or (2) that the radiation comes from a simple dipole photosphere, with a wide range of field strengths represented and possible changes with orbital phase.

a) A Polar Spot at a Single Field?

The first hypothesis may be tested for hydrogen features by comparing wavelengths of the observed absorption with the calculations of Kemic (1974). Figure 9*a* includes estimated curves of important H β and some H γ component positions for field strengths $\gtrsim 20$ megagauss, extended from a diagram in Angel (1978). At low fields, the linear Zeeman effect splits components into three groups having $\Delta m_l = +1, 0,$ and -1 , commonly referred to as σ_- , π , and σ_+ components. Different l -states within each group are separated by the quadratic shift (always blueward) at relatively higher field values. (The orbital l is no longer a good quantum number in the presence of an external field, but it remains a useful designator of the various components having the same Δm_l ; see Kemic 1974.) Thus, the overall hydrogen opacity is spread over a huge wavelength range when the quadratic effect dominates; since the zero-field line is highly saturated in hot white dwarfs, the total equivalent width of H β or H γ may be increased greatly. One curious and important effect of the l -state spreading is that the isolated individual components can no longer be effectively perturbed by Stark ion fields. Thus, for minimal magnetic broadening, sharp absorption features can be found in hot white dwarfs such as Feige 7 (Liebert *et al.* 1978), and we believe that such features are seen in the AM Her spectra.

It is evident from comparing the MMT spectra (Figs. 1, 3, and 9) with the Zeeman component curves that much of the absorption can be explained by hydrogen near a single field strength of 13 megagauss. The strong absorption at 4600–4700 Å may be identified as a

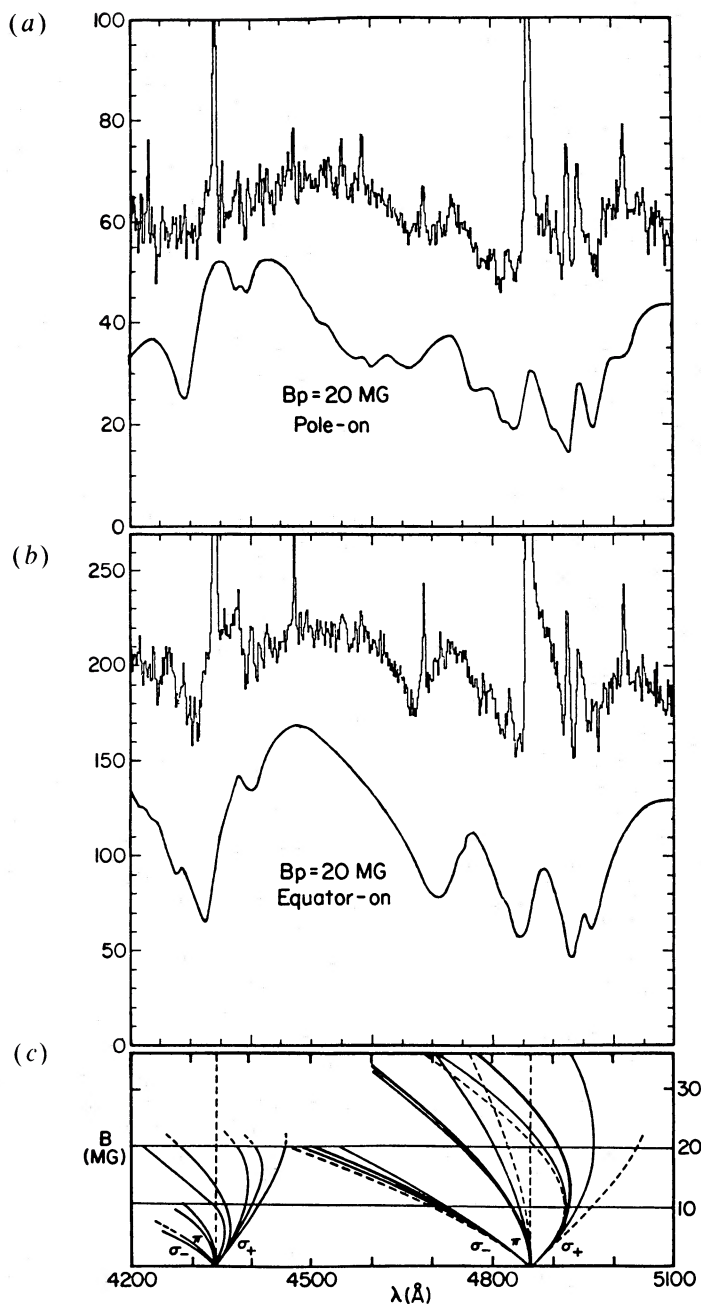


FIG. 9.—(a) A composite spectrum of files 184 and 185 at mean phase 0.97 during which time the emission lines were weak, compared with a synthetic Zeeman spectrum from Wickramasinghe and Martin (1979a) for a magnetic DA star with polar field strength of 20 megagauss, viewed pole-on; (b) a composite spectrum near phase 0.55 (files 202, 203, 215, 229, and 230), again at times when emission lines were relatively weak compared with an equator-on view of the same magnetic DA model; (c) the position of significant $H\beta$ and $H\gamma$ Zeeman components are plotted against surface magnetic field strength for wavelengths and fields relevant to the AM Her spectra. Bold, solid curves have highest statistical weight in Kemic's (1974) compilation, dashed curves have lowest weight.

pile-up of field-sensitive $H\beta$ σ_- components at 13 megagauss. This field strength would also be consistent with identifying the deep absorption minima near 4815 Å and 4840 Å in the mean spectra, with the two $H\beta$ π components having the greatest transition strengths. (These are the $2p-4d$ series in Kemic's notation.) We can conclude that a large fraction of the emitting surface is at a field strength near 13 megagauss.

There are, however, two characteristics in the scans which would require substantially higher field strengths to be present for a purely hydrogen-line interpretation:

First, both the $H\beta$ π and σ_- absorption regions extend further to the blue, with the former evidently reaching as low as 4750 Å. This absorption requires a maximum field of ~ 20 megagauss. The extended σ_- absorption requires $B \gtrsim 15$ megagauss, and this conclusion is consistent with the extended, positive, circular polarization at these wavelengths (Schmidt, Stockman, and Margon 1981). Unfortunately, the superposition of strong TiO band absorption at critical wavelengths prevents any obvious check from the $H\alpha$ profiles.

The second high-field characteristic requires understanding the curious absorption and emission-line pattern redward of the narrow $H\beta$ and $H\gamma$ emission lines. Indeed, the Zeeman absorption is so prevalent throughout the blue wavelength range, it appears that the regions just longward of $H\beta$ and $H\gamma$ and the ~ 4500 Å region offer the nearest thing to true continuum intervals in the MMT spectra. These regions are so elevated in some scans above neighboring absorbed regions, they have the appearance of extended red wings to the narrow emission. However, the differences between the $H\beta$ and $H\gamma$ wing profiles, and the absence of any corresponding features at $H\alpha$ or the helium emission lines, leave little doubt that the wings are not part of the emission profiles. Furthermore, it is untenable to ascribe the extra 4870–4910 Å or 4350–4380 Å radiation to superpositions of additional, weak emission lines. Given the results in § IV, these would have to be low excitation lines, presumably due to such ions as Fe II. Indeed, one might expect some weak contribution from blends dominated by Fe I near $\lambda 4870$, and the He I $\lambda 4388$ line is weakly present. However, as is evident from Figure 8, the total line flux to be accounted for is quite large, especially near phase zero, yet the amount of flux in the wings is *anticorrelated* in phase with the strengths of isolated low excitation emission lines (see § IV). It seems inescapable that the two wing regions are relative maxima in the continuum.

Beyond 4900 Å, the spectra show the strong Fe II/He I blend near 4922 Å and another apparent emission line with a peculiar profile centered near 4945 Å. We have mentioned the secondary's TiO bandhead, and weak Fe I $\lambda 4946$ emission may be contributing. As was the case with the $H\beta$ wing region, however, the total apparent flux interpreted as emission is very large compared with

that observed in strong, isolated, low-excitation emission lines. Furthermore, the 4945 Å profile varies from scan to scan, as does the $H\beta$ wing, though generally showing the same kind of redward skew.

Perusal of the Balmer line Zeeman curves (Fig. 9c) leads us to a plausible explanation of the $H\beta$ and $H\gamma$ wings and the extra continuum near 4945 Å: These are relatively unabsorbed regions between different σ_+ and π components for $H\beta$ and $H\gamma$. Furthermore, the surface field strength must extend much higher than 13 megagauss or these pseudocontinuum regions would actually be much broader in wavelength. Specifically, we note the following:

1. The deep, sharp absorption in the 4960–4990 Å region can be ascribed to the strong $2p_0-4d_{-1}\sigma_+$ component. The required field strength is $\gtrsim 19$ megagauss beyond which the component's position is remarkably insensitive to field strength. This is the range of field at which the quadratic shift succeeds in reversing the direction of the linear shift. Such sharp turnaround components were noted previously in the isolated, magnetic, white dwarf Feige 7 (Liebert *et al.* 1978). They also demonstrate the breakdown of the normal photospheric pressure broadening, due to the magnetic separation of the Stark levels mentioned previously.

2. The pseudocontinuum centered near $\lambda 4945$ is just the region between the $2p_0-4d$ component and the strong absorption due to more field-sensitive σ_+ components (see Fig. 9a).

3. The 4870–4890 Å skewed pseudocontinuum is the region just to the blue of these field-sensitive σ_+ components. The degree to which it is eaten away at its red end should be a sensitive indicator of maximum field strength in the region contributing to the optical light. This maximum field appears to vary with phase, as we will discuss next, and is in the range of 20–22 megagauss.

b) A Dipole Field?

Given that there is evidence for field strengths spanning nearly a factor of 2 (13–21 megagauss) if the Zeeman absorption features are interpreted as purely hydrogen components, it is appropriate to look for phase-dependent variations in the spectra. We must proceed carefully with this, since we have already noted in § IVb and Figure 7 that the absorption feature strengths weakened during an episode of enhanced accretion and may correlate inversely with the strengths of the emission lines. Inspection of the average spectra within phase intervals of 0.2 (Fig. 3) show little evidence for variations in the sharp features, but, if we are correct in our identifications, these turnaround features appear sharp precisely because they are insensitive to field strength anyway. On the other hand, in Figure 9a, b we have summed spectra taken only during periods of relatively weak emission lines (omitting June 18 data)

for phases near 0.55 and 0.97 respectively. There are clear differences between these averages which cannot be explained by variable masking due to a smooth cyclotron continuum. In particular: (1) the field-sensitive $H\gamma$ π components appear deeper or less spread out on the phase 0.55 average; the less field-sensitive $H\beta$ π components vary less. (2) The field-sensitive $H\beta$ σ_- components also appear more confined with a clear minimum near 4660 Å on the phase 0.55 average; they spread more to shorter wavelengths on the phase 0.97 composite. (3) Finally, the $H\beta$ σ_+ components cut more sharply into the 4870–4890 Å pseudocontinuum near phase zero than they do at phase 0.55.

Finally, we noted that the $H\alpha$ absorption near 6300 Å, redward of the main TiO absorption, also appeared sharper for phases ~ 0.5 . Thus we find that all field-sensitive components show clear variations with phase in the sense that, for a purely Balmer line interpretation, there is a strong concentration of a ~ 13 megagauss field near phase 0.55 while this concentration is diluted with more higher field near phase 0. Sums taken at other phases showed that these choices represented the extremes in the shifts of the field-sensitive features.

We thus are led to directly test the second simple-field configuration suggested at the beginning of § VI—that the radiation comes from an entire photosphere with a dipole geometry, like some isolated magnetic white dwarfs. Fortunately, detailed atmospheric synthetic spectra for dipolar DA degenerates have been published by Wickramasinghe and Martin (1979a). In Figure 9a, b we have graphically copied two of these energy distributions onto the scale of our averaged AM Her spectra. The chosen models were for centered dipoles having a polar field strength of 20 megagauss at $T_{\text{eff}} = 12,000$ K, with pole-on ($i=0^\circ$) and equator-on views. The unrealistic temperature choice is not critical given that Wickramasinghe and Martin computed the models using normal Stark broadening. Since it now seems clear that Stark broadening is sharply curtailed for white dwarf photospheres at 10–20 megagauss, we conclude that these calculations should (1) artificially smear the sharper, field-insensitive features, especially the $H\beta$ σ_+ , and (2) produce generally stronger absorption, due to the increased total broadening of highly saturated lines. Accordingly, Wickramasinghe and Martin (1979b) were unable to reproduce the sharper features in Feige 7. Still, the use of a lower-than-realistic model temperature for comparison with AM Her helps compensate for effect (2).

It is apparent that the phase 0.55 spectrum bears some similarity to the equator-on synthetic spectrum, while the 0.97 average shows more high-field features in the direction of the pole-on view. In general, we would not expect any of the phase averages to represent either of the geometric extremes, but rather a range of intermediate inclination angles. The evidence presented by

Bailey and Axon (1981) and this paper in § III suggests that the active pole producing negative circular polarization is at high rotational latitude so that this range could be rather modest. However, scrutiny of the available model spectra suggests that the AM Her absorption may be more complicated than a simple, centered, hydrogen dipole. The absorption near 4700 Å is probably too deep to be fit by any intermediate inclination angle, and there is a predominance of ~ 13 megagauss features at all phases.

There is, in fact, a serious conflict with the suggestion that a magnetic pole is being viewed more directly (i.e., closer to pole-on) at phase 0 than at phase 0.5. Tuohy *et al.* (1981, § VIa) summarize some compelling arguments in favor of an opposite geometry: that the primary (negative) accretion pole is viewed more directly near phase 0.5 and passes briefly behind the primary limb at phase 0. The two main arguments are that (1) the sharp, stable X-ray eclipse and (2) the optical pulse of linear polarization both happen near phase 0 and should occur when the accretion column passes behind the limb of the star (Stockman 1977). Thus for the reasons stated in this and the preceding paragraph, we will consider qualitatively some more complicated models.

c) A Complicated Photosphere?

The possible complications to the field geometry are difficult to assess, particularly if the polar region is highly structured. However, we first consider the possible roles of helium features and temperatures variations.

i) Helium Features?

The appearance of strong Ly α with the high temperature IUE continuum suggested a photospheric $T_{\text{eff}} > 30,000$ K. This indicates He II $\lambda 4686$ could be stronger than the He I line opacities for the intermediate composition “DAO” white dwarfs (cf. Liebert 1980). In fact, strong neutral helium transitions would be possible only if the temperatures were close to 30,000 K. However, the addition of helium features may help resolve the difficulties with the dipole fit outlined in § VIb. In particular, the lack of detailed agreement with the $H\beta$ σ_- components in the 4600–4700 Å region could be due to He II 4686 absorption. This hydrogenic ion has energy shifts close to its hydrogen counterpart $H\beta$ (Garstang 1977). For fields in the 10–20 megagauss range, its π components are concentrated near 4650 Å. Also, we note that the complicated spectrum redward of $H\beta$ might be due in part to He I $\lambda 4921$, which is strong in hot DB white dwarfs (i.e., $T_{\text{eff}} \sim 25,000$ K, with nearly pure helium atmospheres). Is it possible that the combination of He II and He I can explain all of the ~ 20 megagauss features near 4880 Å, 4970 Å and below 4700 Å, so that a polar spot model near 13 megagauss could be valid after all? We do not rule out this possibil-

ity, but note that it would require the helium feature strengths to vary in a rather ad hoc way due to composition and/or temperature changes. There is a specific way of testing the possible opacity due to He I transitions by looking at the relatively isolated He I lines having field-insensitive transitions, particularly the π components of low-level transitions. Such features include the strong $\lambda 5876$ 2^3P-3^3D line, observed in the red data, and the $\lambda 5015$ 2^1S-3^1P line. Neither of these show evidence for π absorption at any phase, nor does the $\lambda 4471$ 2^3P-4^3D line. Thus it is doubtful that the $\lambda 4921$ (2^1P-4^1D) π components produce the strong absorption previously attributed to H β components near 20 megagauss. However, He II $\lambda 4686$ absorption may well explain the lack of a detailed hydrogen dipole fit in the 4600–4700 Å range.

ii) Temperature Variations?

One might expect the polar regions to be considerably hotter than the remaining photosphere, due to the deposition of accretion energy or even localized thermonuclear burning. This leads to the limiting case of a polar hot spot dominating the radiation output, but doesn't readily accommodate the coexistence of strong ~ 13 megagauss features with a phase-variable admixture of apparent higher-field components. If the polar region had $T_{\text{eff}} \gg 30,000$ K, that might be too high for significant Balmer absorption, showing us the polar strength when the pole is viewed most directly. However, polar radiation must surely contribute strongly to the *IUE* continuum, yet the strong Ly α profile suggests T_{eff} nearer the bottom part of Raymond's (1980) allowed range. Furthermore, the pole cannot otherwise be occulted by infalling gas near phase ~ 0.5 (again to mask the higher photospheric field features at this phase), since this would require significant optical depth in the Paschen continuum, for which there is no evidence from the weakened emission lines. Thus, while photospheric temperature variations seem likely to occur, they cannot readily be used to explain the apparent phase-dependence of the magnetic geometry.

iii) Offsetting the Dipole?

It is an open-ended task to consider the possible complexities for an extended, photospheric light source. However, a simple vertical displacement of a dipole center from the primary's center-of-mass may contribute to solving the phase-dependent geometry problem discussed at the end of § VI b. A modest displacement along the polar axis allows the opposite poles to have substantially different field strengths. In particular, we suggest that the positive circular polarization pole which is visible only briefly following zero phase has the higher of the polar field strengths (say 22 megagauss). Thus more high field components contribute near phase zero,

when more or this polar cap is visible, but do not contribute near phase 0.5 when we view all of the negative polar cap at a lower field strength. The broad equatorial value would be 12–13 megagauss, while the negative polar strength might be ~ 18 megagauss. Note that the vertical offset required for polar values of 22 and 18 megagauss is only about 3% of the radius. This would have no appreciable effect far from the star. The dominant accretion is assumed to occur to the negative pole because that pole points more directly toward the secondary in the phase-locked binary picture.

d) Summary

In § VI we have explored in as much detail as possible the Zeeman absorption spectrum. Much of the absorption may be explained by hydrogen in a dominant magnetic field strength near 13 megagauss. However, there are pervasive features which also seem to require either hydrogen magnetic field components near 20 megagauss or a variable and unlikely admixture of neutral helium components. Aside from the masking due to enhanced accretion events, there are also phase-dependent variations in the positions and strengths of the Zeeman absorption components. Thus the spectrum cannot be explained by a simple, heated, polar-spot model, but there are apparent complications beyond a simple dipole photospheric interpretation as well. Furthermore, the stronger contribution of higher field components near phase zero seems incompatible with the geometry inferred from the phase dependence of the linear polarization and the X-rays. We suggest that He II $\lambda 4686$ absorption complicates the dipole fit in the 4600–4700 Å region; this is compatible with temperature estimates from *IUE* data and is consistent with atmospheric studies of hot white dwarfs. Finally, a vertically offset dipole geometry with the higher-field magnetic pole visible only near phase zero might reconcile the geometric difficulties.

We are grateful to Peter Stockman and John Raymond for results in advance of publication, as well as several soul-searching discussions. We thank Ann Cowley and Santiago Tapia for sharing some advance results, Janet Mattei for communicating the invaluable A.A.V.S.O. reports on AM Her, and Pat Boeshaar for her assessment of the secondary spectrum. The successful operation of the MMT spectrograph and photon-counting Reticon system on its maiden voyage in 1980 May–June is due to a large number of people, but especially Roger Angel, Ray Weymann, John Geary, and Dick Young. Thanks are also due to Fred Chaffee and Bill Wyatt for help with the reduced MMT data. J. L. acknowledges support from NSF grant AST 78-021071. J. E. S. acknowledges Fundação de Amparo a Pesquisa do Estado de São Paulo for financial support under contract FAPESP (03)79/0629.

REFERENCES

- Angel, J. R. P. 1978, *Ann. Rev. Astr. Ap.*, **16**, 487.
 Angel, J. R. P., Carswell, R., Strittmatter, P. A., Beaver, E. A., and Harms, R. 1974, *Ap. J. (Letters)*, **194**, L47.
 Angel, J. R. P., Hilliard, R. L., and Weymann, R. J. 1979, in *The MMT and the Future of Ground-based Astronomy*, ed. T. C. Weekes (Smithsonian Astrophysical Observatory Special Report No. 385), p. 87.
 Bailey, J., and Axon, D. J. 1981, *M.N.R.A.S.*, **194**, 189.
 Berg, R., and Duthie, J. 1977, *Ap. J.*, **211**, 859.
 Boeshaar, P. 1976, Ph.D. thesis, Ohio State University, Columbus.
 ———. 1980, private communication.
 Bond, H. E., and Tift, W. G. 1974, *Publ. A.S.P.*, **86**, 981.
 Channugam, G., and Wagner, R. L. 1977, *Ap. J. (Letters)*, **213**, L13.
 Crampton, D., and Cowley, A. P. 1977, *Publ. A.S.P.*, **89**, 374.
 Crampton, D., Hutchings, J. B., and Cowley, A. P. 1981, *Ap. J.*, **243**, 567.
 Fabbiano, G., Hartmann, L., Raymond, J., Steiner, J., Branduardi-Raymont, G., and Matilsky, T. 1981, *Ap. J.*, **243**, 911.
 Feigelson, E., Dexter, L., and Liller, W. 1978, *Ap. J.*, **222**, 263.
 Garstang, R. H. 1977, *Rept. Progr. Phys.*, **40**, 105.
 Greenstein, J. L., and Bokstein, A. 1978, *M.N.R.A.S.*, **185**, 823.
 Greenstein, J. L., Sargent, W. L. W., Boroson, T. A., and Bokstein, A. 1977, *Ap. J. (Letters)*, **218**, L121.
 Hearn, D. R., and Richardson, J. A. 1977, *Ap. J. (Letters)*, **213**, L115.
 Hege, E. K., Cromwell, R. C., and Woolf, N. J. 1979, in *Advances in Electron Physics*, p. 52.
 Kemic, S. B. 1974, *JILA Report*, No. 113.
 Lamb, D. Q. 1976, review talk, Ann Arbor Workshop on AM Herculis, November 1976.
 ———. 1979, in *Compact Galactic X-Ray Sources*, ed. F. K. Lamb and D. Pines (Urbana Ill.: University of Illinois Press), p. 27.
 Lamb, D. Q., and Masters, A. R. 1979, *Ap. J. (Letters)*, **228**, L105.
 Landstreet, J. D. 1979, in *IAU Colloquium 53, White Dwarfs and Variable Degenerate Stars*, ed. V. Weidemann and H. M. Van Horn (Rochester, NY: University of Rochester), p. 297.
 Latham, D. W. 1979, in *The MMT and the Future of Ground-based Astronomy*, ed. T. C. Weekes (Smithsonian Astrophysical Observatory Special Report No. 385), p. 119.
 Liebert, J. 1980, *Ann. Rev. Astr. Ap.*, **18**, 363.
 Liebert, J., Stockman, H. S., Angel, J. R. P., Woolf, J., Hege, E. K., and Margon, B. 1978, *Ap. J.*, **225**, 201.
 Mattei, J. 1980, *IAU Circ.*, No. 3490.
 O'Connell, R. 1973, *A.J.*, **78**, 1074.
 Patterson, J. 1980, *IAU Circ.*, No. 3500.
 Raymond, J. C., Black, J. H., Davis, R. J., Dupree, A. K., Gursky, H., Hartmann, L., and Matilsky, T. A. 1979, *Ap. J. (Letters)*, **230**, L95.
 Raymond, J. 1980, private communication.
 Robinson, E. L. 1976, *Ann. Rev. Astr. Ap.*, **14**, 119.
 Schmidt, G. D., Stockman, H. S., and Margon, B. 1981, *Ap. J. (Letters)*, **243**, L157.
 Schneider, D. P., and Young, P. 1980, *Ap. J.*, **240**, 871.
 Stockman, H. S. 1977, *Ap. J. (Letters)*, **218**, L57.
 Stockman, H. S., Liebert, J., and Bond, H. E. 1979, in *IAU Colloquium 53, White Dwarfs and Variable Degenerate Stars*, ed. V. Weidemann and H. M. Van Horn (Rochester, NY: University of Rochester), p. 334.
 Stockman, H. S., and Sargent, T. A. 1979, *Ap. J.*, **227**, 197.
 Stockman, H. S., Schmidt, G. D., Angel, J. R. P., Liebert, J., Tapia, S., and Beaver, E. A. 1977, *Ap. J.*, **217**, 815.
 Tapia, S. 1977a, *Ap. J. (Letters)*, **212**, L125.
 ———. 1977b, *IAU Circ.*, No. 3054.
 ———. 1980, private communication.
 Tuohy, I. R., Mason, K. O., Garmire, G. P., and Lamb, F. K. 1981, *Ap. J.*, **245**, 183.
 Visvanathan, N., and Wickramasinghe, D. T. 1979a, *Nature*, **281**, 47.
 ———. 1979b, in *IAU Colloquium 53, White Dwarfs and Variable Degenerate Stars*, ed. V. Weidemann and H. M. Van Horn (Rochester, NY: University of Rochester), p. 330.
 Wickramasinghe, D. T., and Martin, B. 1979a, *M.N.R.A.S.*, **188**, 165.
 ———. 1979b, in *IAU Colloquium 53, White Dwarfs and Variable Degenerate Stars*, ed. V. Weidemann and H. M. Van Horn (Rochester, NY: University of Rochester), p. 317.
 Young, P., and Schneider, D. P. 1979, *Ap. J.*, **230**, 502.

DAVID W. LATHAM and JOÃO E. STEINER: Harvard-Smithsonian Center for Astrophysics, 60 Garden Street, Cambridge, MA 02138

JAMES LIEBERT: Steward Observatory, University of Arizona, Tucson, AZ 84721